Kinematics modeling and analysis of four degrees of freedom carrying manipulator trajectory

Lijun Wang, Guangchao Zhang, Hao Ren, Weijie Wu

School of Mechanical Engineering,
North China University of Water Resources and Electric Power,
Zhengzhou 450011, Henan, China

Abstract
In this paper, combining with the examples, we focus on the study of general Kinematics modeling and simulation of Four degrees of freedom carrying manipulator based on laboratory development. On the basis of calculating kinematic positive and inverse solutions, a space trajectory curve is planed which is composed of three sections of straight lines and two pieces of circular arc. For 4R manipulator trajectory planning, the researchers propose a polynomial interpolation method based on displacement at the end of the tool in the joint space. The method is applicable to any power of polynomial interpolation and simplifies the complex curve and the process of trajectory planning. In this paper, we make a simulation of 4R manipulator movement by using Adams, and realize the expected results. Besides, by analyzing the results, some shortcomings have been found, which may need further research.
Key words: 4R SERIAL MANIPULATORS, KINEMATICS ANALYSIS, TRAJECTORY PALNNING, NUMERICAL SIMULATION

Introduction

Industrial robots (IR) are the ability to independent action and multi-axis linkage of mechanical equipment. Today they have been a lot of application in industrial production, especially in automotive manufacturing. The online programming, automatic control, humanoid operating characteristics makes it get application in space, medicine, agriculture, etc gradually [1]. But the inverse solution in spatial structure, trajectory tracking control, the optimal time control, and repetitive positioning accuracy are still big deficiency. To solve these problems, it has accumulated a lot of research results at home and abroad [2].

Industrial robot system is a complicated multi-input and multi-output nonlinear system. It is connected with time-varying, strong coupling and nonlinear dynamics, so the control problem is very complicated. An accurate mathematical model is difficult to obtain using conventional techniques. Therefore, an efficient technique is required to deal with these types of complex and dynamic systems. R.D.,Al-Dabbagh proposed to use Fuzzy Adaptive DE (FADE) algorithm, and through the simulation to prove that this algorithm is more efficient than the traditional algorithm [3]. The generality of the industrial manipulators architecture, there is no single established explicit solution. M.A.,González-Palacios introduced a classification of anthropomorphic, while considered sixteen different architectures whose inverse kinematics are solved with a single approach [4]. Hamid T and Mohammad F put forward an adaptive method to

solve the inverse kinematics problem of redundant manipulator [5]. They used neural network to obtain a cartesian coordinate system of the joint Angle, and using the quadratic programming to meet the constraints, and improved neural network. Lin Xiao and Yunong Zhang wanted to obtain the accurate solution of the time-varying inverse kinematics for mobile manipulators, so a special class of recurrent neural network, named Zhang neural network (ZNN), is exploited and investigated [6]. This algorithm compared with the traditional algorithm has obvious advantages. Manipulator trajectory planning can be in joint space and cartesian space, and it need to consider the path and obstacle constraints when it is running in space. Philipp Ennen et al. put forward a kind of effective method of collision avoidance when industrial robots work in the overlap area [7]. Due to mechanical arm end need to complete predefined multiple tasks in the shortest time, and in the process of movement need to consider obstacle avoidance, the order is difficult to identify. Paraskevi Th. Zacharia et al. introduced a method for simultaneously planning collision-free motion and scheduling time-optimal route along a set of given task-points [8]. There are many joint trajectory planning methods, e.g., three times polynomial interpolation, path points of three times polynomial interpolation, excessive linear high-order polynomial interpolation, parabolic interpolation and parabola linear interpolation path points, etc. Shafaat Ahmed Bazaz used a low-order polynomial method to realize the optimal time control of industrial manipulator real-time trajectory [9]. Industrial production of cooperation between the many tasks need more arms to complete, at this time, not only need to consider each technical specifications of the mechanical arm, and also need to be combined with the specific task for motion planning [10]. M.H. Korayem, S.R. Nekoo investigates finite-time optimal and suboptimal controls for time-varying systems with state and control nonlinearities [11]. To complete a task if the time is certain, it will need to through the precise trajectory tracking to assign accurate time to the task of every step, which would require the mechanical arm has higher positioning accuracy. Industry usually adopts some sensors for calibration at the end of the manipulator trajectory. Commonly used laser tracker is quite expensive, so low-cost measurement system and tools of industrial mechanical arm are very important [12]. In the design stage of the mechanical arm needs to test its running status under the variety of complex environment. Using virtual prototype can reduce the physical test of mechanical arm, reducing development cycle and cost [13]. Based on the kinematics analysis and numerical simulation of the virtual prototype of mechanical arm, it can make an accurate and rational assessment of the rigid and flexible mechanical arm.

A cubic polynomial interpolation method based on displacement at the end is proposed in this paper. The coordinate transformation of the mechanical arm is analyzed by using D-H method. Even though there are a lot of trajectories within the range which the end of the mechanical arm can reach, as long as the typical trajectory can be realized, the other complex trajectories can be realized just with some slight differences from each other in the aspect of the complexity of the algorithm. The corresponding amount of calculation and computational complexity is different from each other by using different interpolation methods, and different track smoothness and motion stability will be shown. Therefore, a cubic polynomial interpolation method is adopted in this paper. At first the Solidworks is used to draw the 3d model and then the Adams is imported to make simulation analysis in order to verify the correctness of trajectory planning and algorithm.

Kinematic modeling

Mechanical arm 3d model in Adams and simulation curve at the end of trajectory is shown in figure 1. According to the 3d model of 4R manipulator in figure 1, each link coordinate system manipulator can be obtained in figure 2:

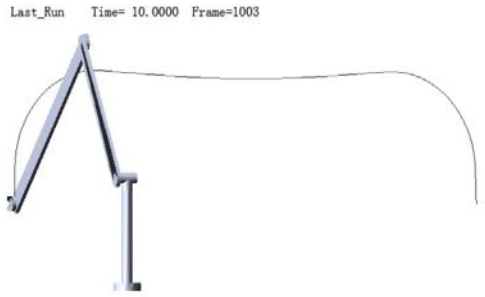

Figure 1. 3d model and the simulation curve

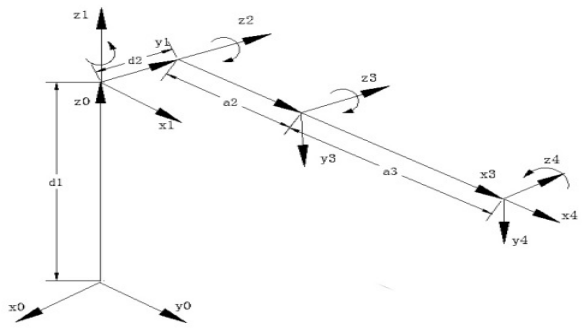

Figure 2. D-H link coordinate system

In figure 2, the manipulator's D-H link parameters established by using the D-H method are shown in table 1:

Table 1. 6R Manipulator's D-H connecting rod parameter, mm

Joint number	θ_i	α_{i-1}	a_{i-1}	d_i
1	90°	0		620
2	0	−90°		50
3	0	0	500	
4	0	0	800	

By the above parameters, positive kinematics of manipulator can be solved.

According to table 1 and the connecting rod transformation is given, (In the formula 1, ,$s\theta_i = \sin\theta_i, c\theta_i = \cos\theta_i, c_i = \cos\theta_i, s_i = \sin\theta i$)

$$ {}^{i-1}_{i}T = \begin{pmatrix} c\theta_i & -s\theta_i & 0 & a_{i-1} \\ s\theta_i c\alpha_{i-1} & c\theta_i c\alpha_{i-1} & -s\alpha_{i-1} & -d_i s\alpha_{i-1} \\ s\theta_i s\alpha_{i-1} & c\theta_i s\alpha_{i-1} & c\alpha_{i-1} & d_i c\alpha_{i-1} \\ 0 & 0 & 0 & 1 \end{pmatrix} \quad (1) $$

Get the manipulator's each link coordinate system as follows:

$$ {}^{0}_{1}T = \begin{pmatrix} c_1 & -s_1 & 0 & 0 \\ s_1 & c_1 & 0 & 0 \\ 0 & 0 & 1 & d_1 \\ 0 & 0 & 0 & 1 \end{pmatrix} \quad (2) $$

$$ {}^{1}_{2}T = \begin{pmatrix} c_2 & -s_2 & 0 & 0 \\ 0 & 0 & 1 & d_2 \\ -s_2 & -c_2 & 1 & 0 \\ 0 & 0 & 0 & 1 \end{pmatrix} \quad (3) $$

$$ {}^{2}_{3}\mathrm{T} = \begin{pmatrix} c_3 & -s_3 & 0 & a_2 \\ s_3 & c_3 & 0 & 0 \\ 0 & 0 & 1 & 0 \\ 0 & 0 & 0 & 1 \end{pmatrix} \quad (4) $$

$$ {}^{3}_{4}T = \begin{pmatrix} c_4 & -s_4 & 0 & a_3 \\ s_4 & c_4 & 0 & 0 \\ 0 & 0 & 1 & 0 \\ 0 & 0 & 0 & 1 \end{pmatrix} \quad (5) $$

Each connecting rod transformation matrix is multiplied, the manipulator's transformation matrix ${}^{0}_{4}T$ can be got.

Namely: ${}^{0}_{4}T = {}^{0}_{1}T(\theta_1){}^{1}_{2}T(\theta_2){}^{2}_{3}T(\theta_3){}^{3}_{4}T(\theta_4)$. It is the function of each joint variable: $\theta_1, \theta_2, \theta_3, \theta_4$, Now solve the manipulator's motion equation (In the formula, $c_{34} = c_3c_4 - s_3s_4, s_{34} = c_3s_4 + s_3c_4$)

$$ {}^{0}_{2}T = {}^{0}_{1}T{}^{1}_{2}T = \begin{pmatrix} c_1c_2 & -c_1s_2 & -s_1 & -s_1d_2 \\ s_1c_2 & -s_1s_2 & c_1 & c_1d_2 \\ -s_2 & -c_2 & 0 & d_1 \\ 0 & 0 & 0 & 1 \end{pmatrix} \quad (6) $$

$$ {}^{2}_{4}T = {}^{2}_{3}T{}^{3}_{4}T = \begin{pmatrix} c_{34} & -s_{34} & 0 & c_3a_3+a_2 \\ s_{34} & c_{34} & 0 & s_3a_3 \\ 0 & 0 & 1 & 0 \\ 0 & 0 & 0 & 1 \end{pmatrix} \quad (7) $$

$$ {}^{0}_{4}T = {}^{0}_{2}T{}^{2}_{4}T = \begin{pmatrix} c_1c_2c_{34} - c_1s_2s_{34} & -c_1c_2s_{34} - c_1s_2c_{34} & -s_1 & c_1c_2(c_3a_3 + a_2) - c_1s_2s_3a_3 - s_1d_2 \\ s_1c_2c_{34} - s_1s_2s_{34} & -s_1c_2s_{34} - s_1s_2c_{34} & c_1 & s_1c_2(c_3a_3 + a_2) - s_1s_2s_3a_3 + c_1d_2 \\ -s_2c_{34} - c_2s_{34} & s_2s_{34} - c_2c_{34} & 0 & -s_2(c_3a_3 + a_2) - c_2s_3a_3 + d_1 \\ 0 & 0 & 0 & 0 \end{pmatrix} \quad (8) $$

On the expression of wrist transformation matrix, the connecting rod coordinate system{4} relative to the situation is described at the end of the position{0}. Check the applicability of ${}^{0}_{4}T$, when $\theta_1 = 90°, \theta_2 = \theta_3 = \theta_4 = 0$, at the end of the wrist transformation matrix has a value of ${}^{0}_{4}T$.

$$ {}^{0}_{4}T = \begin{pmatrix} 0 & 0 & -1 & -d_2 \\ 1 & 0 & 0 & a_3 + a_2 \\ 0 & -1 & 0 & d_1 \\ 0 & 0 & 0 & 1 \end{pmatrix} \quad (9) $$

Be consistent with the case shown in figure.

Now for the inverse kinematics of manipulator, first of all, ${}^{1}_{4}T$ can be got:

$$ {}^{1}_{4}T = {}^{1}_{2}T{}^{2}_{4}T = \begin{pmatrix} c_2c_{34} - s_2s_{34} & -c_2s_{34} - s_2c_{34} & 0 & c_2(c_3a_3 + a_2) - s_2s_3a_3 \\ 0 & 0 & 1 & d_2 \\ -s_2c_{34} - c_2s_{34} & s_2s_{34} - c_2c_{34} & 0 & -s_2(c_3a_3 + a_2) - c_2s_3a_3 \\ 0 & 0 & 0 & 1 \end{pmatrix} \quad (10) $$

Set

$$ {}^{0}_{4}T = \begin{pmatrix} n_x & o_x & a_x & p_x \\ n_y & o_y & a_y & p_y \\ n_z & o_z & a_z & p_z \\ 0 & 0 & 0 & 1 \end{pmatrix} $$

So

${}^{0}_{1}\mathrm{T}^{-1}(\theta_1){}^{0}_{4}\mathrm{T} = {}^{1}_{4}\mathrm{T} = {}^{1}_{2}\mathrm{T}(\theta_2){}^{2}_{3}\mathrm{T}(\theta_3){}^{3}_{4}\mathrm{T}(\theta_4)$

Then each joint variable can be solved：

$$\begin{pmatrix} c_1 & s_1 & 0 & 0 \\ -s_1 & c_1 & 0 & 0 \\ 0 & 0 & 1 & -d_1 \\ 0 & 0 & 0 & 1 \end{pmatrix}\begin{pmatrix} n_x & o_x & a_x & p_x \\ n_y & o_y & a_y & p_y \\ n_z & o_z & a_z & p_z \\ 0 & 0 & 0 & 1 \end{pmatrix} = {}^1_4T \quad (11)$$

The element(2,4) is equal on both sides of the matrix equation,

$$-s_1 p_x + c_1 p_y = d_2 \quad (12)$$

$$\left.\begin{aligned} \mathrm{c_1p_x + s_1p_y = c_2(c_3a_3 + a_2) - s_2s_3a_3 = a_3c_{23} + a_2c_2} \\ \mathrm{-p_z + d_1 = -s_2(c_3a_3 + a_2) - c_2s_3a_3 = a_3s_{23} + a_2s_2} \end{aligned}\right\} \quad (14)$$

gain $\theta_3 = \mathrm{acos\ (k)}$ (15)

In the formula 15, $\mathrm{k} = (p_x^2 + p_y^2 - d_2^2 + (p_z - d_1)^2 - a_2^2 - a_3^2)/2a_2a_3$

In the formula 15, the element(1,4) and(2,4) are equal on both sides of the matrix equation.

By

$$\left.\begin{aligned} c_1c_{23}p_x + s_1c_{23}p_y - s_{23}p_z + s_{23}d_1 - a_2c_3 = a_3 \\ -c_1s_{23}p_x - s_1s_{23}p_y - c_{23}p_x + c_{23}d_1 + a_2s_3 = 0 \end{aligned}\right\} \quad (17)$$

gains

$$\begin{cases} s_{23} = \dfrac{a_2s_3(c_1p_x+s_1p_y)+(a_2c_3+a_3)(d_1-p_z)}{(c_1p_x+s_1p_y)^2+(d_1-p_z)^2} \\ c_{23} = \dfrac{(c_1p_x+s_1p_y)(a_2c_3+a_3)-a_2s_3(d_1-p_z)}{(c_1p_x+s_1p_y)^2+(d_1-p_z)^2} \end{cases} \quad (18)$$

namely $\theta_{23} = \theta_2 + \theta_3$ (19)

$$\theta_{23} = \mathrm{atan2}\begin{bmatrix} a_2s_3(c_1p_x + s_1p_y) + (a_2c_3 + a_3)(d_1 - p_z), \\ (c_1p_x + s_1p_y)(a_2c_3 + a_3) - a_2s_3(d_1 - p_z) \end{bmatrix}$$

$$\theta_2 = \theta_{23} - \theta_3 \quad (20)$$

gain

$$\theta_1 = \mathrm{atan2}(p_y, p_x) - \mathrm{atan2}(d_2, \pm\sqrt{p_x^2 + p_y^2 - d_2^2}) \quad (13)$$

By

By ${}^0_3T^{-1}(\theta_1, \theta_2, \theta_3){}^0_4T = {}^3_4T(\theta_4)$

Gain

$$\begin{pmatrix} c_1c_{23} & s_1c_{23} & -s_{23} & s_{23}d_1 - a_2c_3 \\ -c_1s_{23} & -s_1s_{23} & -c_{23} & c_{23}d_1 + a_2s_3 \\ -s_1 & c_1 & 0 & -d_2 \\ 0 & 0 & 0 & 1 \end{pmatrix}\begin{pmatrix} n_x & o_x & a_x & p_x \\ n_y & o_y & a_y & p_y \\ n_z & o_z & a_z & p_z \\ 0 & 0 & 0 & 1 \end{pmatrix} = {}^3_4T \quad (16)$$

In addition, due to the need to guarantee that the manipulator end always stays in the process of sports level, $\theta_4$can be obtained.

Namely $\theta_4 = \theta_2 + \theta_3$ (21)

Above all, all joints variables have been calculated, formula 11-21 are the results. In formula 13, plus or minus is about different steering joints. Through the actual investigation, the formula of a plus sign is more reasonable. According to the above results, trajectory planning, simulation and post-processing are studied.

Tool trajectory planning at the end

Mechanical arm needs to implement handling functions, so tool path in the space is set at three sections of straight line and two pieces of arc. The hand vertical rises from A to B, and then through the circular arc transition to point C, and horizontal motion to point D, and through the circular arc transition to point E, and then smooth vertical down to the point of F. Specific lines and dimensions are shown in figure 3:

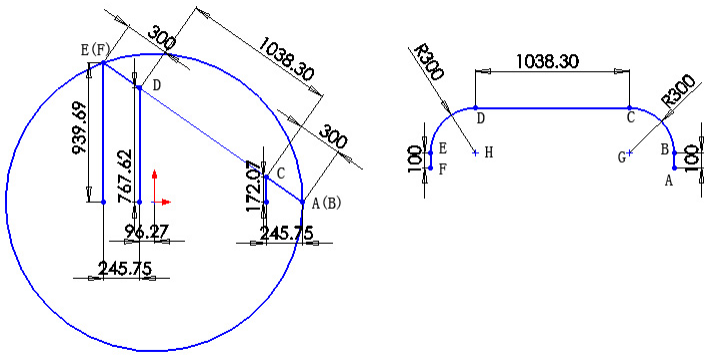

Figure 3. Trajectory curve view (left) and front view (right)

Five space curve equation is shown as follows:

$$\begin{cases} l_{AB} & x=-50, y=1000, z=520+t_{1(0\le t_1\le 100)} \\ l_{BC} & \begin{cases} 172.07(y-1000)-245.75(x+50)=0_{(-50\le x\le -222.07)} \\ (x+222.07)^2+(y-754.25)^2+(z-620)^2=300^2 \end{cases} \\ l_{CD} & 172.07(y-1000)-245.75(x+50)=0_{(-817.62\le x\le -222.07)}, z=920 \\ l_{DE} & \begin{cases} 172.07(y-1000)-245.75(x+50)=0_{(-989.69\le 0\le -817.62)} \\ (x+817.62)^2+(y+96.27)^2+(z-620)^2=300^2 \end{cases} \\ l_{EF} & x=989.69, y=-342.02, z=520+t_{2(0\le t_2\le 100)} \end{cases} \quad (22)$$

Now, we can propose an improved cubic polynomial interpolation method for interpolation calculation. First of all, straighten the whole trajectory curve as a straight line, the total distance of S. According to the initial velocity(v_0) and the terminate velocity(v_0) and the time(T) during the operation, the three times polynomial coefficients can be obtained. Then equal division of time, and calculate the displacement of each time point, then calculate the coordinates of each section of the displacement, according to coordinate values and formula (14) - (21) calculate the joint variables of each point in time. At the junction of straight and arc calculate the speed and time point respectively, and then can respectively calculate the path points of each curve. Ensure that each curve of equal value of the same time, so that the end of the mechanical arm displacement, velocity and angular velocity continuously can ensure smooth operation in the process of the whole mechanical arm. Combined with the design of the mechanical arm, cubic polynomial of displacement and time is as follows:

$$s(t) = a_0 + a_1 t + a_2 t^2 + a_3 t^3 \quad (23)$$

When t=0, the initial displacement $S(0)=a_0=0$, initial velocity $v_0=a_1$. Again by the total distance S and terminate velocity v_t, a_2, a_3 can be calculated. In this design of the T = 10 s, S = 2180.78 mm, $a_0 = a_1 = 0, a_2 = 65.4234\text{mm}, a_3 = -4.3625\text{mm}$

Taking a series of points of curve in Cartesian space as the point of path, gain table 2.

Table 2. The end of the tool' path point and joint Angle

Time, sec	Coordinate values, mm			Angle value, rad			
	x	y	z	θ_1	θ_2	θ_3	θ_4
0.01	-50	1000	520.000000	-0.000004	-0.000001	0.000028	0.000027
0.02	-50	1000	520.000000	-0.000004	-0.000008	0.000030	0.000022
0.03	-50	1000	520.026134	-0.000004	-0.000031	0.000035	0.000004
0.04	-50	1000	520.058763	-0.000004	-0.000069	0.000043	-0.000026
…	…	…	…	…	…	…	…
3.37	-223.454926	752.268188	919.507751	0.224979	-0.747153	0.386472	-0.360681
3.38	-225.130569	749.875000	919.507751	0.227753	-0.750774	0.390129	-0.360645
3.39	-226.808655	747.478333	919.507751	0.230545	-0.754389	0.393772	-0.360617
3.40	-228.489151	745.078247	919.507751	0.233354	-0.758000	0.397402	-0.360598
…	…	…	…	…	…	…	…
6.67	-818.473267	-97.533508	919.493561	1.631467	-0.665124	0.301429	-0.363695
6.68	-820.143799	-99.919395	919.451099	1.634221	-0.661268	0.297413	-0.363855
6.69	-821.811523	-102.301231	919.380488	1.636958	-0.657396	0.293406	-0.363990
6.70	-823.476257	-104.678795	919.281864	1.639676	-0.653509	0.289409	-0.364100

…	…	…	…	…	…	…	…
9.97	-988.868958	-340.892670	517.694319	1.854939	0.078522	-0.117654	-0.039132
9.98	-988.868958	-340.892670	517.648664	1.854939	0.078573	-0.117666	-0.039093
9.99	-988.868958	-340.892670	517.615950	1.854939	0.078610	-0.117675	-0.039065
10.00	-988.868958	-340.892670	517.596418	1.854939	0.078632	-0.117680	-0.039048

The simulation results

In Adams, the spline function is generated from joint parameters of table 2, then the spline function input in the drive of each joint is simulated. The result is shown in figure 4. It can be found that the end of the tool path is consistent with the planning. If it is further analyzed, all images can be obtained when running the tool tip. The displacement curve, velocity curve and angular velocity curve of the end of tool operation obtained through simulation are shown in the figure.

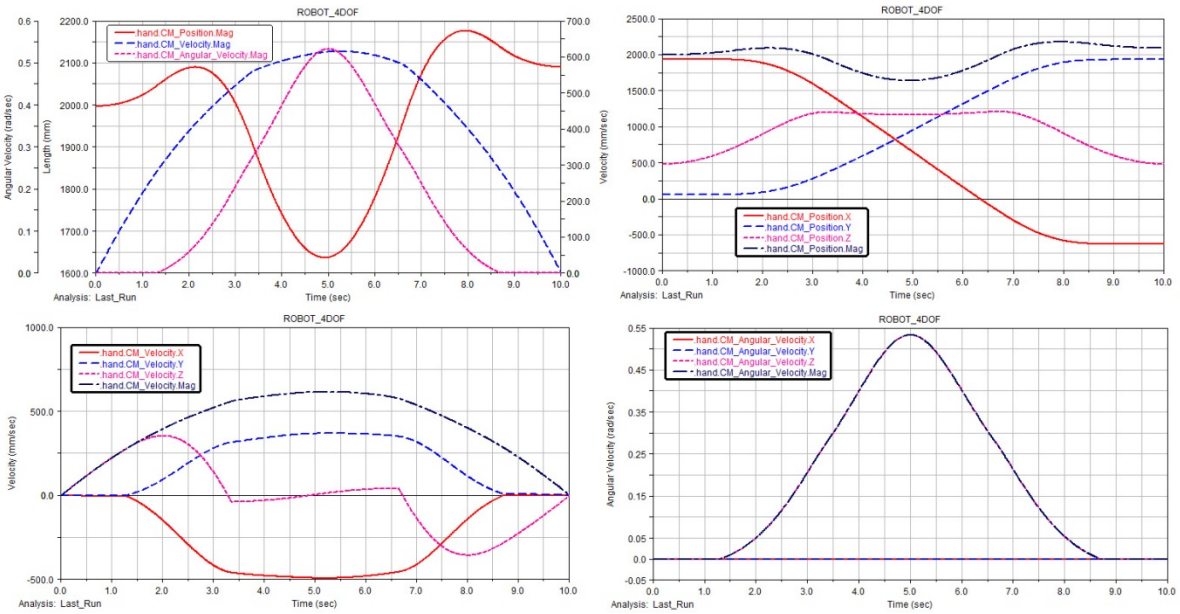

Figure 4. The end of the tool axis and comprehensive curve

Each figure of the above can determine displacement, velocity and angular velocity of the end of the mechanical arm in the process of movement along the axis of motion and comprehensive sports meet the basic requirements, and mechanical arm terminal operation process is very smooth to verify the effectiveness of the improved cubic polynomial interpolation method.

The end of the tool along the x axis and y axis the angular velocity curve shown in figure5:

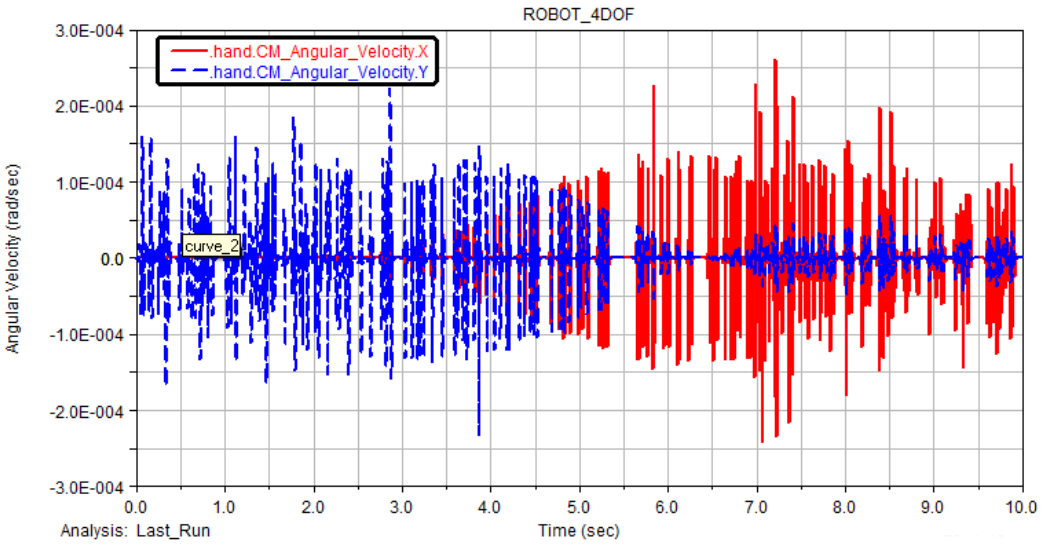

Figure 5. The end of the tool along the x and y axis angular velocity curve

In figure 5, the angular velocity curve has a real-time fluctuation. Fluctuating value mostly is controlled between -0.0001rad/sec and +0.0001rad/sec, so the mechanical arm angular velocity fully meet the design requirements.

In addition, the angle acceleration curve of mechanical arm is as follows.

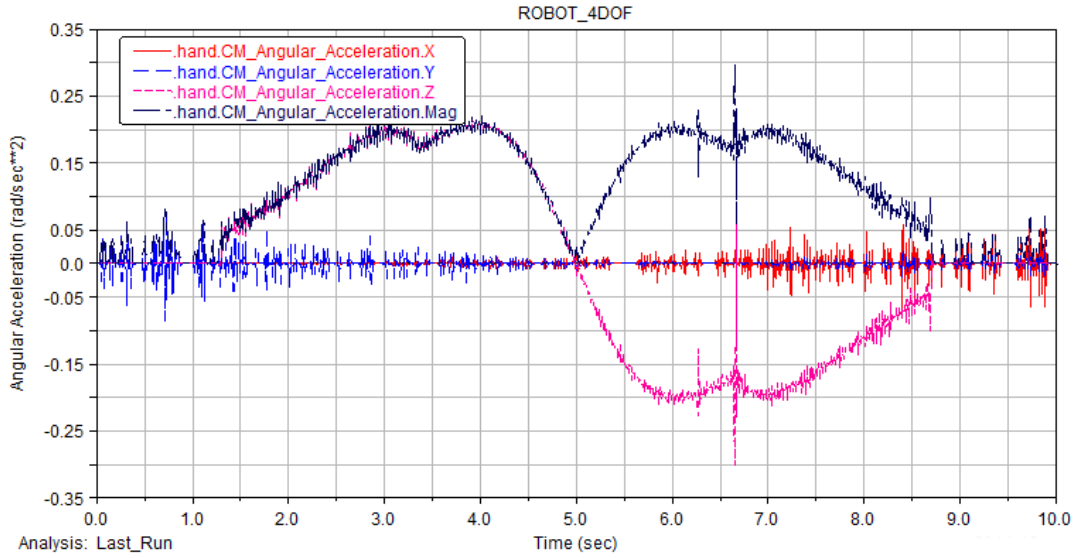

Figure 6. The end of the tool axis and comprehensive angular acceleration curve

The figure 6 shows that the angular acceleration was in fluctuation condition, which is related to the approximate calculation in the process of operation. In addition, angular acceleration at two curves connecting has a big step, which is related to two curve connecting path point values. On the whole the end of tool' displacement, velocity, angular velocity and angular acceleration fluctuation is not big, if the curve of the joint trajectory planning is made by using higher order interpolation, the displacement, velocity and acceleration fluctuation will be smaller.

Discussion and conclusion

For 4R manipulator, after the 3D model is set up, D-H parameters are used to determine the D-H link parameters of mechanical arm, and then mechanical arm kinematics equation is got according to the linkage parameters, and then the kinematics inverse solution of mechanical arm is solved. In order to verify whether the mechanical arm can complete the task successfully within the planned space, a circular arc transition curve is given in three-dimensional space. In order to make the movement effect more stable, the displacement of the modified cubic polynomial interpolation

method is put forward to plan trajectory in joint space on the basis of traditional cubic polynomial interpolation method. This approach can be used for calculating any curve by adjusting the sampling period to ensure that the cohesion point of every two curve has been taken, which can weaken the cohesion point acceleration jump so as to ensure the smooth of displacement and velocity. At the same time, if the other higher order interpolation method is used, this method still works very well and the resulting mechanical arm movement velocity and acceleration performance will be better. Finally, according to the method and formula in the Adams simulation, the expected results are obtained. The simulation results also confirm what is said about the correctness of the modeling and kinematics analysis of mechanical arm. Based on this method, any posture of complex mechanical arm movement will be realized in the three-dimensional space within the scope the manipulator can reach. At the same time, it should be noted that there is a shortcoming of this method that the running time cannot be changed after it is set. In addition, the acceleration images show a wave phenomenon, and it becomes more obvious in the linkage between the two curves. If the running time can be planned more reasonably, decreasing the sampling period can reduce the influence of the results.

Acknowledgements

This work was supported by Zhengzhou Measuring & Control Technology and Instrumentations Key Laboratory(121PYFZX181) and HASTIT(14HASTIT001)

References

1. Remzi S. , Ahmet Y.M. (2014) A New Robot for Flexible Ureteroscopy: Development and Early Clinical Results (IDEAL Stage 1-2b). *European Urology*, 66(6), p.p.1092-1100
2. G LEENA, G RAY. (2012) A set of decentralized PID controllers for an n-link robot manipulator. *Sadhana*, 37(3), p.p.405-423
3. Rawaa D.A., Azeddien K., Saad M. (2014) System identification and control of robot manipulator based on fuzzy adaptive differential evolution algorithm. *Advances in Engineering Software*, 78, p.p.60-66
4. Max A.G. (2013) The unified orthogonal architecture of industrial serial manipulators. *Robotics and Computer-Integrated Manufacturing*, 29(1), p.p.257-271
5. Hamid T., Mohammad F. (2014) Real-time inverse kinematics of redundant manipulators using neural networks and quadratic programming. *A Lyapunov-based approach, Robotics and Autonomous Systems*, 62(6), p.p.766-781
6. Lin X., Yunong Z. (2014) Solving time-varying inverse kinematics problem of wheeled mobile manipulators using Zhang neural network with exponential convergence. *Nonlinear Dynamics*, 76(2), p.p.1543-1559
7. Philipp E., Daniel E., Daniel S., Sabina J. (2014) Efficient Collision Avoidance for Industrial Manipulators with Overlapping Workspaces. *The International Academy for Production Engineering*, 20, p.p.62-66
8. Paraskevi Th. Zacharia, Elias K. (2013) Aspragathos, Task scheduling and motion planning for an industrial manipulator. *Robotics and Computer-Integrated Manufacturing*, 29(6), p.p.449-462
9. Shafaat A.B., Author V., Bertrand T. (1999) Minimum time on-line joint trajectory generator based on low order spline method for industrial manipulators. *Robotics and Autonomous Systems*, 29(4), p.p.257-268
10. F.Basilea, F.Caccavaleb, P.Chiacchioa (2012) Task-oriented motion planning for multi-arm robotic systems. *Robotics and Computer-Integrated Manufacturing*, 28(5), p.p.569-582
11. M.H. Korayem, S.R. Nekoo (2015) Finite-time state-dependent Riccati equation for time-varying nonaffine systems: Rigid and flexible joint manipulator control. *ISA Transactions*, 54(1), p.p.125-144
12. Giovanni L., Monica T. (2014) Optimal design and application of a low-cost wire-sensor system for the kinematic calibration of industrial manipulators. *Mechanism and Machine Theory*, 73, p.p.25-48
13. N. Prabhua, M. Dev Anandb, S. Rajac (2012) Development of a CAD Based Platform for Scorbot-ER Vu Industrial Robot Manipulator. *Procedia Engineering*, 38, p.p.3992-3997.